Surface Wave Propagation in Thin Silver and Aluminium Films

Anouar Njeh[a], Nabil Abdelmoula[b], Hartmut Fuess[c], and Mohamed Hédi Ben Ghozlen[b]

[a] Institut Préparatoire aux Etudes d'Ingénieurs de Sfax, BP 805, 3018 Sfax, Tunisia
[b] Laboratoire de Physique de Matériaux, Faculté des Sciences, Université de Sfax, 3018 Sfax, Tunisia
[c] Institute of Materials Science, University of Technology, Petersenstr. 23, D-64287 Darmstadt, Germany

Reprint requests to Dr. A. N.; Fax: +216-74-243542; E-mail: njehanouar@yahoo.fr

Three kinds of acoustic waves are known: bulk waves, pseudo-surface waves and surface waves. A plane wave section of a constant-frequency surface of a film serves as a hint for the expected nature. Calculations based on slowness curves of films reveal frequency ranges where each type of acoustic waves is predominant. Dispersion curves and displacement acoustic waves are calculated and commented in each frequency interval for different coated materials. Both dispersion and sagittal elliptical displacement are sensitive and depend on diagrams mentioned above. Silver and aluminium thin films having different anisotropy ratios, namely 2.91 and 1.21, are retained for illustration.

Key words: Surface Acoustic Waves; Propagation; Dispersion; Thin Films; Mechanical Properties.

1. Introduction

The preparation of solid films requires the understanding of their mechanical properties. Such films are parts of microelectronic devices and improve the hardness and wear resistance of coatings.

Surface acoustic waves (SAWs) are convenient tools to study the mechanical properties of thin films, because the rate of their energy away from the surface is frequency-dependent. With increasing SAW frequency, the energy is concentrated closer into the surface. Therefore the influence of the elastic properties of the film on the velocity increases as well [1 – 4].

In coated material the velocity of SAWs depends on their frequency, i. e. shows dispersion. The wavelength, frequency and thickness of the layer are varied to obtain dispersion curves of the SAW. The elastic properties are then derived from these dispersion curves [5].

In anisotropic media the speed of acoustic waves varies with the propagation direction. Particularly, directions exist where the lowest speed of a quasi-transverse bulk wave approaches the speed of SAWs [6, 7].

The purpose of this paper is to describe the dependence of SAWs in Ag/Si and Al/Si systems on the propagation direction and the anisotropy of the material. Special attention is given to SAW displacements: The analysis includes mainly its elliptical characteristics.

2. Surface Acoustic Wave Analysis

An ultrasonic surface wave propagates at the surface of a homogenous material with an amplitude that decreases exponentially perpendicular to the surface and vanishes to negligible values within a few wavelengths below the surface [8]. The penetration depth decreases with increasing frequency. The velocity of propagation is somewhat smaller than the bulk shear velocity associated with the material, which is the same for all frequencies. If the material is coated with a film which has different elastic parameters, the surface wave will become dispersive.

We are going to concentrate on the acoustic properties of an anisotropic solid layer of thickness h, which is perfectly bound to a semi-infinite anisotropic substrate.

We use the coordinate system shown in Fig. 1, with the x_1 and x_2 axis lying in the interface between the layer and the substrate, the x_3 axis being directed into the substrate. Here, the plane with $x_3 = 0$ is the interface between the layer and the substrate, while the plane with $x_3 = -h$ is the free surface. The ultrasonic surface wave propagates along the x_1 axis. The wave must satisfy the appropriate wave equation in the layer and the substrate, and the boundary conditions imposed by the interface and the free surface. The wave equation for the particle displacement in a perfectly elastic and homogeneous medium can be written, in
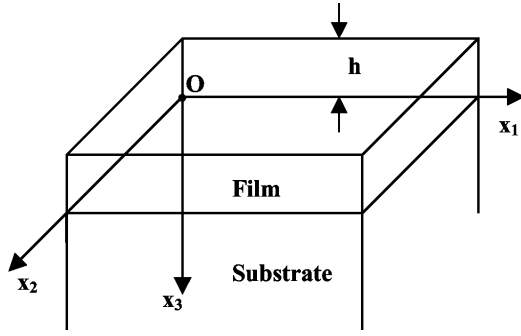
Fig. 1. Coordinate system for surface acoustic waves propagation in a thin film.

the absence of body forces and piezoelectric effects, as [7]

$$\rho \frac{\partial^2 u_i}{\partial t^2} = \mathbf{C}_{ijkl} \frac{\partial^2 u_k}{\partial x_j \partial x_l}, \quad (i,j,k,l = 1,2,3), \quad (1)$$

in which ρ is the density of the medium and $\mathbf{C}_{ijkl}$ is the elastic tensor. The components in (1) refer to the coordinate system of Fig. 1, and the summation convention on repeated subscripts is implied.

In the following, a quantity carrying a tilde designates a quantity of the film and the same quantity without a tilde refers to the substrate. Thus, $\tilde{\rho}$ and $\tilde{\mathbf{C}}_{ijkl}$ are the density and the elastic tensor of the layer material, whereas ρ and $\mathbf{C}_{ijkl}$ are the density and the elastic tensor of the substrate. We assume a straight crested surface wave propagating in the x_1 direction with

$$u_j = u_{0j} \exp(ik\beta x_3) \exp[i(kx_1 - \omega t)], \quad (2)$$

where the components of the wave vector $\vec{k}(k_1 = k, k_2 = 0, k_3 = k\beta)$, the angular frequency ω and the components of the polarisation vector $\vec{u}_0$ are related through the set of three linear equations [9]

$$(\mathbf{C}_{ijkl} k_i k_l - \rho \omega^2 \delta_{jk}) u_{0j} = 0, \quad i,j,k,l = 1,2,3, \quad (3)$$

for which the secular equation is

$$|\mathbf{C}_{ijkl} k_i k_l - \rho \omega^2 \delta_{jk}| = 0, \quad i,j,k,l = 1,2,3. \quad (4)$$

For a given k and ω (4) is of the order 6 in β and may be solved for the six roots $\beta^{(n)}$ ($n = 1$ to 6). The six roots for β are either real or occur in complex conjugate pairs. All six roots are used for the calculation of the film displacement, but only the three roots with positive imaginary parts are taken for the substrate displacement.

Writing the displacements as linear combinations of terms having the phase velocity v, the displacement field in the layer is given as [7, 10]:

$$\tilde{u}_j = \left[\sum_n \tilde{A}_n \tilde{u}_{0j}^{(n)} \exp(ik\tilde{\beta}^{(n)} x_3)\right] \exp[ik(x_1 - vt)], \quad (5)$$
$$n = 1 \text{ to } 6,$$

and in the substrate as:

$$u_j = \left[\sum_m A_m u_{0j}^{(m)} \exp(ik\beta^{(m)} x_3)\right] \exp[ik(x_1 - vt)],$$
$$m = 1,3,5. \quad (6)$$

The coefficients A_m with even subscript m are omitted because they are not related to finite solutions. $\tilde{u}_{0j}^{(n)}$ and $u_{0j}^{(m)}$ are the complex eigenvectors associated with (3) for the film and for the substrate. $\tilde{A}_n$ and A_m are the weighting factors for the linear combination of waves in the film (5) and the substrate (6). Only one eigenvector exists for each root β. $\tilde{u}_{0j}^{(n)}$ and $u_{0j}^{(m)}$ are the components of the eigenvector corresponding to the eigen values $\tilde{\rho} v^2$ and ρv^2, respectively. The weighting factors must be determined by the application of the boundary conditions based on the displacements in (5) and (6). The particle displacements and the traction components caused by the stress components of the wave (T_{13}, T_{23} and T_{33}) must be continuous across the interface under the assumption of a rigid contact between the two materials. Since the free surface is considered to be mechanically stressed free, the three traction components of stress must vanish thereon, and nine boundary conditions are obtained. In order to obtain nontrivial solutions of this set of homogenous equations, the $9 \cdot 9$ determinant of the coefficients $\tilde{A}_n$ and A_m must vanish [7].

3. Results

In this paper cubic symmetry of the film is assumed. The substrate is a single-crystal Si(001) and the wave vector is defined as $x_1 = [100]$. We consider both a thin silver and a thin aluminum film of 200 nm thickness, and two different wave propagation directions are investigated. These are [100], the Xp_1 axis, and [110], the Xp_2 axis. For both configurations, the (001) plane for the film corresponds to the interface film/substrate, and two configurations Ag[100]/Si[100] and Ag[110]/Si[100] are analyzed for an SAW excited along [100] in the substrate.
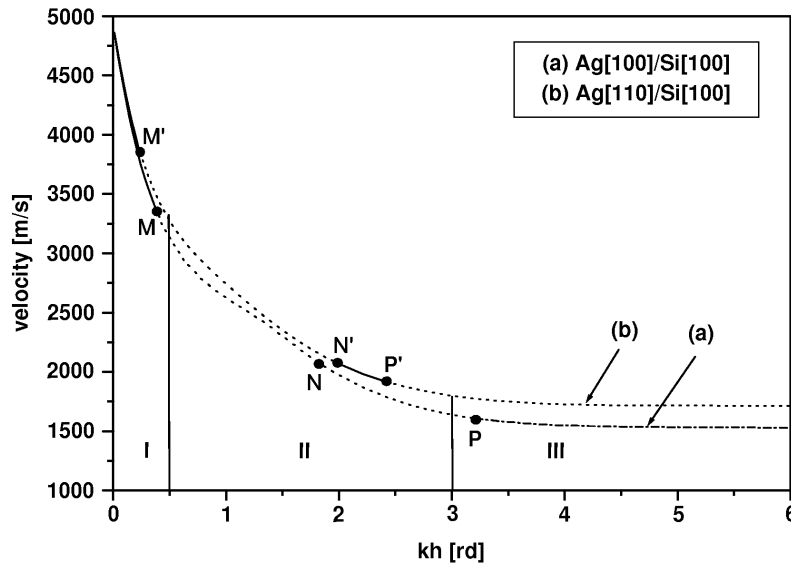
Fig. 2. Surface acoustic wave (SAW) velocity of the first Rayleigh mode in an Ag/Si(001) layered system as a function of the product kh, where k is wave number and h is thickness of the film: (a) the wave propagates along the $Xp_1 = [100]$ axis into the Ag film; (b) the wave propagates parallel to the $Xp_2 = [110]$ axis into the Ag film.

Table 1. Anisotropic materials parameters.

Material	C_{11} [GPa]	C_{12} [GPa]	C_{44}[GPa]	ρ [kg/m³]
Silicon	165.5	63.9	79.5	2329
Aluminum	107.3	60.8	28.3	2702
Silver	123	92	45.3	10500

The determination of the dispersive curves was based on the elastic characteristics reported in Table 1 [11].

3.1. Calculation of the Surface Acoustic Wave Velocity

In this section we apply the theory described above. A silver and aluminum thin film with anisotropic ratios of 2.91 and 1.21, respectively, are used for illustration. The anisotropic ratio is defined as $C_{11} - C_{12}/2C_{44}$. We consider a surface wave propagation along the symmetry axis, Xp_1 or Xp_2 in the (001) plane. By the tentative calculation, one intends to examine the velocity Rayleigh mismatch consequences and the anisotropy impact on dispersion phenomena curves.

For thin films (Ag or Al) grown on silicon, the acoustic waves can be excited and propagate in the film or in the substrate. The film acts as a perturbing parameter on the wave propagation velocity. The velocity change depends on the layer thickness, acoustic frequency and impedance mismatch between layer and substrate.

For the computation of SAW velocities a value of the SAW velocity v is chosen and substituted into (4)

for film and substrate. In a second step the boundary conditions determinant is evaluated. The phase velocity v is iteratively varied until this determinant approaches zero. Repeated for each frequency, the SAW dispersion curves for the thin film coated crystal are obtained.

In Fig. 2, the SAW velocities of the first Rayleigh mode, calculated at various frequencies for an Ag film grown on the (001) plane of the Si substrate, are displayed as functions of kh. Here $h = 200$ nm is the film thickness and k is the wave number. In Fig. 2a we present the dispersion curve for an SAW propagating along the Xp_1 axis, and Fig. 2b corresponds to the dispersion curve along the Xp_2 direction. The velocity shift is sensitive to the normalized thickness. The velocity of the SAW is slightly higher for the Xp_2 direction than for Xp_1.

The dispersion curve shows three sections related to kh values:

Below $kh = 0.5$ rd (region I), the velocity shift is very small and the slope is steep. The film thickness is smaller than the SAW wave length. The wave penetrates the film into the substrate. So, the Rayleigh wave is mainly determined by elastic parameters of Si.

The second region II (for 0.5 rd $\leq kh \leq 3$ rd) is characterized by a higher velocity shift than before. The slope of the dispersion curve decreases. This intermediate region describes the Rayleigh velocity change vs. frequencies from the substrate to the film. This frequency area seems best suited to distin-
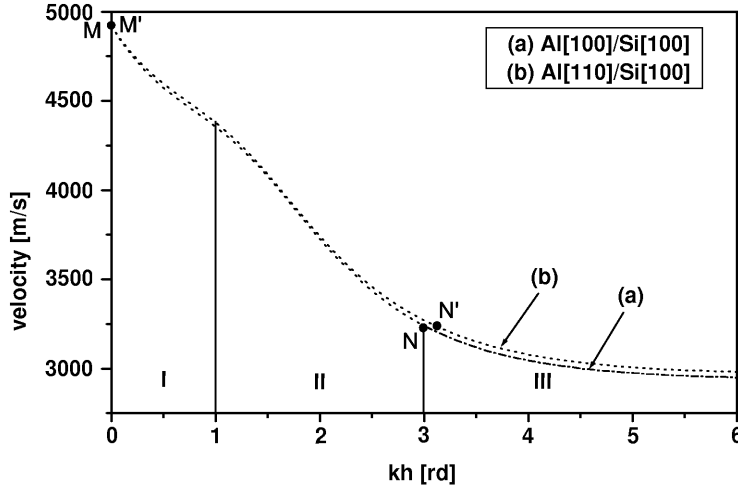
Fig. 3. Phase velocity of the first Rayleigh mode in the Al/Si(001) layered system as a function of the wave number-thickness product kh: (a) the wave propagates along the $Xp_1 = [100]$ axis into the Al film; (b) the wave propagates parallel to the $Xp_2 = [110]$ axis into the Al film.
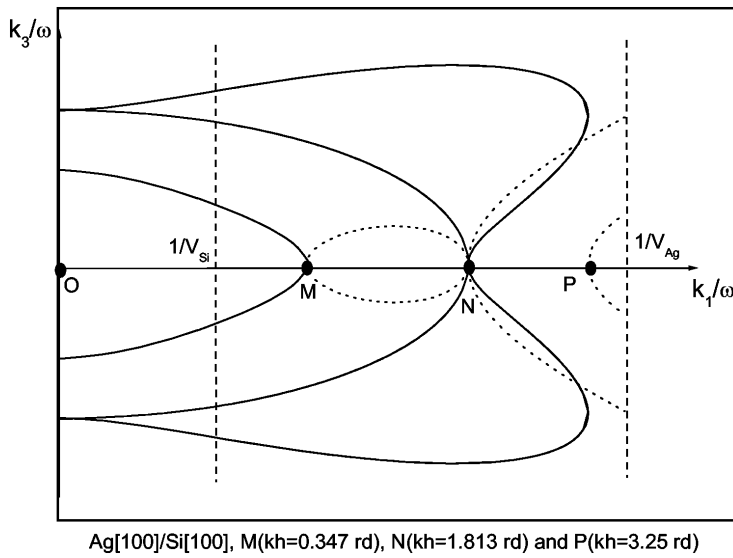

Ag[100]/Si[100], M(kh=0.347 rd), N(kh=1.813 rd) and P(kh=3.25 rd)

Fig. 4. A plane section of a constant frequency surface of an Ag/Si system; k_3/ω as a function of k_1/ω ($k_1 = k$ and $k_3 = \tilde{\beta}k$). (001) is the interface between the Ag film and the Si substrate. The wave propagates along $Xp_1 = [100]$ into the Ag film.

guish between films grown on the first or the second setting.

The region III reveals a slope close to zero and a nearly constant velocity shift. When the exciting frequency increases, the Rayleigh wave is completely localized within the Ag film and its velocity is exclusively dependent on the film characteristics.

Figure 3 displays the dispersion curves for an Al film on a Si(001) substrate. Due to the small anisotropic ratio for aluminum, the shift between the velocities of the surface waves propagating along Xp_1 and Xp_2 is smaller than for Ag and the mismatch is different. Dispersion curves reveal three areas with different slope. The second region, defined for 1 rd $\leq kh \leq$ 3 rd, presents a higher slope than the first ($kh \leq 1$ rd) and the third region ($kh \geq 3$ rd). The calculated curves are sensitive to the film anisotropic ratio and to the Rayleigh velocity mismatch.

3.2. Plane Wave Section of a Constant-frequency Surface

We are now dealing with generated waves propagating along Xp_1 and Xp_2 within the film. At this level and for a given Rayleigh velocity v, the parameters $\tilde{u}_{0j}^{(n)}$, $\tilde{\beta}^{(n)}$ and $\tilde{A}_n$ are calculated on the basis of standard methods [1, 7]. For a given frequency, (4) has six solutions $\tilde{\beta}^{(n)}$, $n = 1, \ldots, 6$. Real solutions correspond
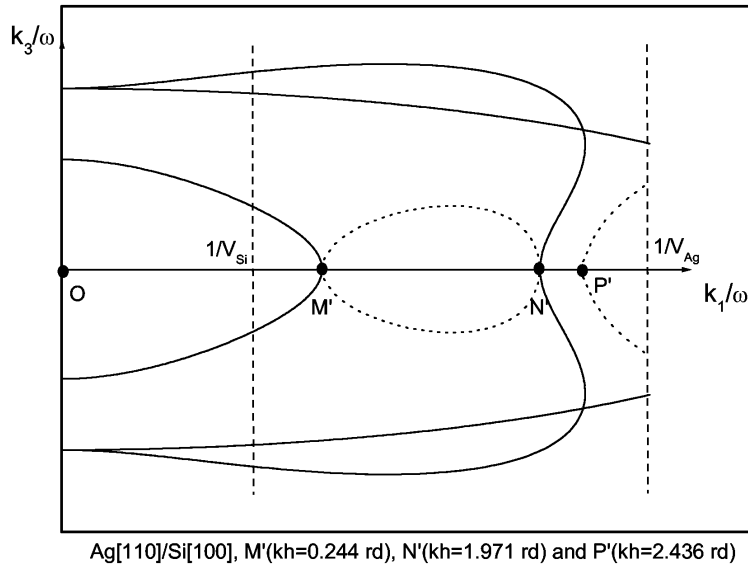
Fig. 5. A plane section of a constant frequency surface of an Ag/Si system; k_3/ω as a function of k_1/ω ($k_1 = k$ and $k_3 = \tilde{\beta}k$). (001) is the interface between the Ag film and the Si substrate. The wave propagates along $Xp_2 = [110]$ into the Ag film.

Ag[110]/Si[100], M'(kh=0.244 rd), N'(kh=1.971 rd) and P'(kh=2.436 rd)

to bulk homogeneous plane waves, whereas complex solutions correspond to inhomogeneous ones [7, 10].

Figure 4 displays a plane wave section of a constant-frequency surface of the Ag film. We note that a surface wave propagates along Xp_1 with a velocity between V_{Si} and V_{Ag} (V_{Si} and V_{Ag} are the velocities of the Rayleigh wave for free surface silicon and for free surface silver). Solid lines represent the real solutions whereas the imaginary part is visualized by dotted ones. It is obvious from this figure how the bulk waves, longitudinal (L), fast transverse (FT) and slow transverse (ST), vary with direction. The points M, N and P, correspond to $kh = 0.347$ rd, 1.813 rd and 3.25 rd and present the values of k with complex solutions. The region between O and P is known as the supersonic region [7].

For 0 rd $\leq kh \leq 0.347$ rd the wave in the Ag film consists of three bulk acoustic waves [solid curve in Fig. 2a] and between M and P (0.347 rd $\leq kh \leq 3.25$ rd) of two transverse bulk waves associated with an evanescent wave [dotted curve in Fig. 2a]. Point P is known as the transonic state. Beyond P ($kh > 3.25$ rd) the subsonic region starts where all solutions are complex. So, the surface acoustic wave consists of three evanescent waves and propagates with the velocity of the Rayleigh wave for the free silver surface [dot-dashed curve in Fig. 2a]. The elastic energy is concentrated in the film.

The plane wave section of a constant-frequency surface is presented in Fig. 5 for a wave which propagates along Xp_2 in the Ag film. The frequencies of the surface wave correspond to $kh = 0.244$ rd (point M') and $kh = 2.436$ rd (point P').

For 0 rd $\leq kh \leq 0.244$ rd and for 1.971 rd (point N') $\leq kh \leq 2.436$ rd, three bulk acoustic waves appear [solid curve in Fig. 2b]. For other kh values, the wave consists of evanescent waves associated with bulk waves. In particular, for $kh > 2.436$ rd, two of the partial waves are evanescent while the third has a bulk-like nature which radiates the energy into the substrate. This is called pseudo-surface acoustic wave (p-SAW). The p-SAW is similar to Rayleigh waves (RWs), also sagitally polarized, but with a shorter lifetime and leaking energy onto the substrate when the propagation direction is slightly tilted from Xp_2 [3]. The Rayleigh surface acoustic wave exists in the range 0 to 30 degrees from the Xp_1 direction, while the p-SAW ranges between 0 and 20 degrees from the Xp_2 direction [6, 12].

Similar diagrams have been plotted for the Al/Si heterostructure. The aluminum film is almost isotropic, and different sequences are expected. First, we consider an acoustic wave propagating along the Xp_1 axis in the Al/Si system. A plane wave section of a constant-frequency surface of this system is presented in Fig. 6. For $kh \geq 0$ rd ($v \geq V_{Si}$) the surface wave appears, and for $kh \leq 3.022$ rd it decomposes in two bulk waves associated with an evanescent one [dotted curve in Fig. 3a]. For $kh \geq 3.022$ rd, only complex solutions exist and the RW propagates in the aluminum film in
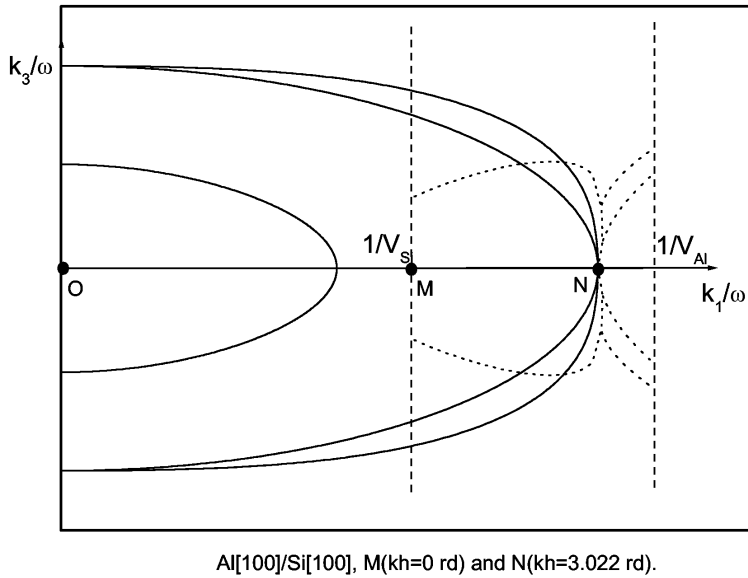
Al[100]/Si[100], M(kh=0 rd) and N(kh=3.022 rd).

Fig. 6. A plane section of a constant frequency surface of an Al/Si system; k_3/ω as a function of k_1/ω ($k_1 = k$ and $k_3 = \tilde{\beta}k$). (001) is the interface between the Al film and the Si substrate. The wave propagates along $Xp_1 = [100]$ into the Al film.
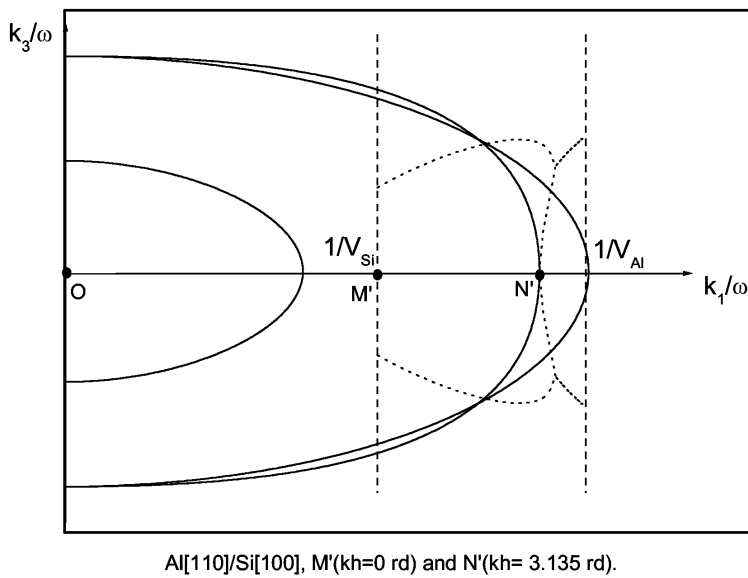

Al[110]/Si[100], M'(kh=0 rd) and N'(kh= 3.135 rd).

Fig. 7. A plane section of a constant frequency surface of an Al/Si system; k_3/ω as a function of k_1/ω ($k_1 = k$ and $k_3 = \tilde{\beta}k$). (001) is the interface between the Al film and the Si substrate. The wave propagates along $Xp_1 = [110]$ into the Al film.

the range 0 to 30 degrees from the Xp_1 direction. For the wave propagating along Xp_2 in the Al film, two solutions are present. When the wave propagation direction is slightly tilted from the Xp_2 axis, only pseudo-surface acoustic waves can propagate in the system (Fig. 7).

The above analysis shows four different interfaces, which are able to develop a system of dispersive surface acoustic waves. The diagrams, drawn on the basis of real and complex film slowness in relation to the sagital plane, reveal a description of the expected surface acoustic waves. Around a normalized thickness, the characteristics of surface acoustic waves corresponding to one interface are depicted.

3.3. Elliptical Form of the Resultant Particle Displacement

In coated materials, Rayleigh-type waves exist in high symmetry directions which display the same characteristics as pure Rayleigh waves: At each depth, the difference of phase of the vertical and longitudinal
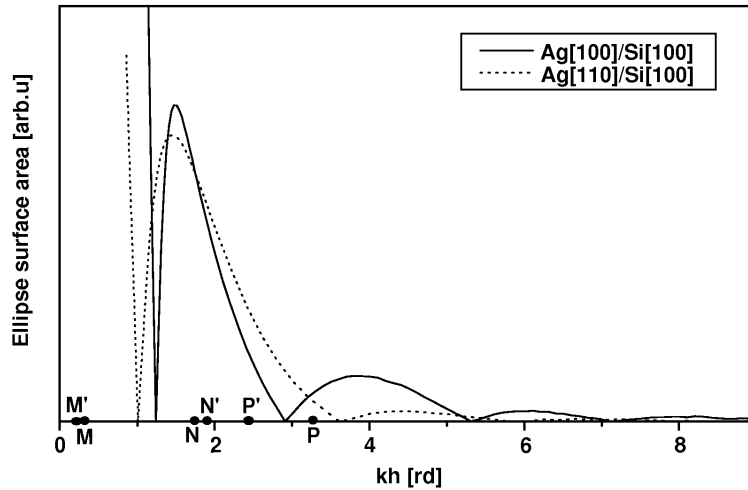
Fig. 8. Variation of the ellipse surface area of the particle displacement amplitude as a function of kh. The Rayleigh-type wave propagates along the Xp_1 axis (solid curves) and along the Xp_2 axis (dotted curves) in the Ag/Si system.

components is equal to $\pi/2$, so that the resultant particle displacement is of elliptical form and the two principal axes of each ellipse are, respectively, longitudinal and vertical [13]. At this level, two kinds of particle displacement are expected: progressive and retrogressive ones. The aim of this paragraph is to describe the oscillation ellipse for a given penetration depth vs the kh parameter for various Rayleigh-type waves.

For pure Rayleigh waves, elliptical displacements do not undergo a change of frequency since the structure is not dispersive. However, a change is observed when the penetration depth is increased. Calculations performed on SAWs reveal that the displacement amplitude decreases with penetration depth. The Rayleigh-type waves behave like pure Rayleigh waves for coated materials. The elliptical oscillations depend not only on the penetration depth, but also on the frequency of the wave excitation.

The Ag/Si system is retained for illustration. On the free film surface, i. e. $x_3 = -h$, and for any frequency, the oscillation ellipse of the particle displacement is retrogressive. For a given penetration depth, i. e. $x_3 > -h$, and for low frequencies, the ellipse moves with retrogressive form. If the frequencies increase, the ellipse has an opposite sense of rotation and changes to progressive. When the frequencies increase further, this behavior changes and the ellipse rotation sense varies.

Figure 8 displays the variation of the ellipse surface of the particle displacements versus the product kh. These surfaces are calculated at the interface, i. e. $x_3 = 0$. Rayleigh-type waves propagate along the Xp_1 axis or the Xp_2 axis in the Ag/Si system. The displacement amplitudes are arbitrarily normalized so that $\tilde{u}_3$ is unity

at the free surface. By increasing the frequency at fixed layer thickness, the product kh increases. As a result, one of the particle displacement amplitudes vanishes. The ellipse surface disappears and the oscillation has an opposite sense of rotation. This behavior is present for $kh = 1.23$ rd, 2.9 rd, 5.34 rd, 7.26 rd and 9.5 rd for propagation along the Xp_1 axis and for $kh = 1.01$ rd, 3.72 rd, 5.94 rd and 7.37 rd for propagation along the Xp_2 axis.

These results can be derived from the plane wave section of a constant-frequency surface of the Ag film. We mentioned before that a surface wave propagating in the Ag/Si system with a velocity between V_{Si} and V_{Ag}, i. e., $\frac{k_1}{\omega}$ ranges between $\frac{1}{V_{Si}}$ and $\frac{1}{V_{Ag}}$ (see Figs. 4 and 5).

When the waves propagate along the Xp_1 axis into the Ag film, complex solutions of k appear for $kh \geq 0.347$ rd (point M) and the corresponding ellipse rotation sense changes in this frequency range. However, the obtained solutions of k are real for $kh < 0.347$ rd and calculated displacements describe an exclusively retrogressive ellipse. For waves propagating along the Xp_2 direction, associated with the Ag film, the real form of the k wave vector is obtained for $kh < 0.244$ rd (point M'). The same behavior is observed for kh values between 1.971 rd (point N') and 2.436 rd (point P'). In these two kh intervals, no change of the ellipse rotation sense is noticed. The change of ellipse rotation is encountered in the following ranges of kh: 0.244 rd $\leq kh \leq$ 1.971 rd and $kh \geq$ 2.436 rd, where imaginary solutions of k appear. In summary, we conclude that the ellipse rotation change is related to a change in the frequency diagram.

4. Conclusions

Two kinds of guided waves, such as Rayleigh waves and pseudo-acoustic waves exist in thin supported layers. The velocity shift is sensitive to the normalized thickness: In the first region, the velocity shift is very small and the slope of the dispersion curve is steep. The second region is characterized by a higher velocity shift than before. The last region reveals a slope close to zero and a velocity shift which is nearly constant.

Plane wave sections of a constant-frequency surface of Ag film or Al film show three ranges of *kh* where the character of the surface wave is different. In the first range, the acoustic wave in the film consists of three bulk waves. An evanescent partial wave appears in the second range of *kh*. Beyond a given value of *kh*, the surface acoustic wave consists of three evanescent waves, and it propagates with the velocity of the Rayleigh wave for the free surface solid. For the Si substrate, the plane wave section of a constant-frequency surface shows that only the evanescent surface wave can propagate.

The rotation sense of the displacement ellipse depends on depth penetration and on wave frequency excitation. From the plane wave section of a constant frequency surface one can detect ranges of frequency where the ellipse oscillation changes from a retrogressive form to a progressive one, or inverse. These ranges correspond to frequency intervals where the evanescent wave in the film exists. Experiments, on the basis of laser surface acoustic waves equipment, have to be undertaken to check and comment on the reported results.

[1] G. W. Farnell and E. L. Adler, Phys. Acoust. **9**, 35 (1972).

[2] D. C. Hurley, V. K. Tewary, and A. J. Richards, Thin Solid Films **398 – 399**, 326 (2001).

[3] E. Chilla, A. V. Osetrov, and R. Koch, Phys. Rev. B **63**, 113308 (2001).

[4] A. Njeh, T. Wieder, D. Schneider, H. Fuess, and M. H. Ben Ghozlen, Z. Naturforsch. **57a**, 58 (2002).

[5] O. Leufeuvre, P. Zinin, and A. D. Briggs, Appl. Phys. Lett. **72**, 856 (1998).

[6] J. O. Kim and J. D. Achenbach, Thin Solid Films **214**, 25 (1992).

[7] A. G. Every, Meas. Sci. Technol. **13**, R21 (2002).

[8] D. Schneider and T. Schwarz, Surf. Coat. Technol. **91**, 136 (1997).

[9] Q. B. Zhou, S. Y. Zhang, and Y. K. Lü, Mater. Sci. Eng. **B83**, 249 (2001).

[10] R. E. Kumon and M. F. Hamilton, J. Acoust. Soc. Am. **113**, 1293 (2003).

[11] Landolt-Börnstein, Neue Serie, III 29/a: Low Frequency Properties of Dielectric Crystals: Elastic Constants (Ed. D. F. Nelson), Springer-Verlag, Berlin, Heidelberg 1992.

[12] J. O. Kim and J. D. Achenbach, J. Appl. Phys. **72**, 1805 (1992).

[13] P. U. Voigt and R. Koch, J. Appl. Phys. **92**, 7160 (2002).